ACS OMEGA

Open Access

http://pubs.acs.org/journal/acsodf

Article

Direct Screening of PET Hydrolase Activity in Culture Medium Based on Turbidity Reduction

Yui Ogura, Yoshihito Hashino, and Akihiko Nakamura*

Cite This: *ACS Omega* 2024, 9, 34151−34160

Read Online

ACCESS | Metrics & More | Article Recommendations | Supporting Information

ABSTRACT: The development of an efficient screening method for the activity of PET-degrading enzymes represents a significant technological advance in the field of enzyme research, with the potential to facilitate the advancement of enzymes for PET recycling. By examining the stable conditions of PET suspension and enzyme production conditions, we developed a method to quantify PET-degrading enzyme activity in *E. coli* culture medium using turbidity reduction as an indicator. High PET concentration or ionic strength caused aggregation of PET, and the best condition for activity detection was 0.5 mg mL^{-1} PET in 50 mM sodium phosphate pH 7.0. Preculture of *E. coli* increased the purity of enzyme secreted in medium. To evaluate the screening method, 720 colonies of the PET2-7M-H229X-F233X mutant library were analyzed and three candidates of high-activity mutants were obtained. The thermostability of the mutants could also be easily measured by measuring the residual activity after heat treatment. The H229T-F233M mutant showed 3.4 times higher degradation rate against PET film than the template enzyme at the initial time. The molecular dynamics simulation implied that the F233M mutation makes space for making an α helix and that the H229T mutation resolved the steric hindrance with Trp199. These mutations were speculated to change the angle of the Trp199 side chain of PET2 to an angle similar to that of the Trp185 of IsPETase, making it suitable for PET binding to the active center. Screening of activity using PET suspensions is compatible with robotic automation and is expected to be useful for validating computationally predicted mutations.

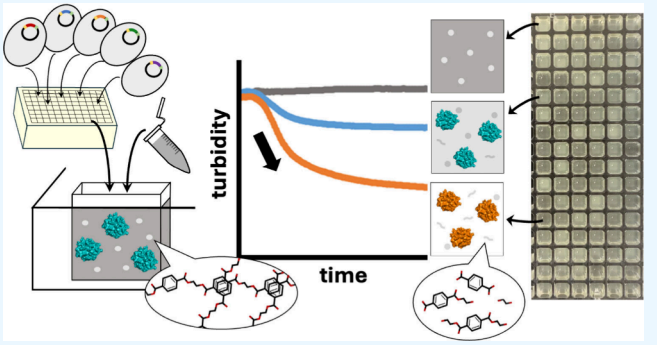

INTRODUCTION

Polyethylene terephthalate (PET) is a polymer of terephthalic acid and ethylene glycol. PET is a very good material with high gas barrier properties, moldability, and chemical resistance.[1,2] Therefore, PET is one of the most popular plastics and commonly used as beverage bottles, clothes, and packages. However, the problem is that these products are used for a short period of time and a large amount of waste is generated.[3] To build a sustainable society in the future, methods to recycle or upconvert PET wastes with minimal environmental impact as much as possible will be necessary.[4]

Recently, enzymatic methods of PET depolymerization have been proposed,[5] and PET-degrading enzymes have been actively developed for this purpose.[6] PET hydrolases have an α/β-hydrolase fold and have 6 helixes and 8 strands in the core structure.[7] This fold is common for many kinds of hydrolases like lipase, protease, and esterase.[8] The three residues Ser, His, and Asp at the active center are called a catalytic triad. The Ser residue attacks the carbon atom of the ester bond and forms a substrate−enzyme intermediate (acylation step).[9] The intermediate is resolved by hydrolysis and returns to its initial state (deacylation step). This reaction cycle is similar to that of serine proteases and lipases.[10,11]

PET hydrolases are classified into three main groups.[7] One is the Type I group, which includes cutinases, degrading the wax layer of plants.[12] Type II is further classified into two subgroups, Type IIa containing lipases and Type IIb containing IsPETase from *Ideonella sakaiensis*, which can grow on PET as a nutrient source.[13] Cutinases have high thermostability and are the enzyme group closest to practical application.[14] Representative enzymes are[15] Cut190 from the actinomycetes *Saccharomonospora viridis*[16] and leaf and branch compost cutinase (LCC) from the compost metagenome library.[17] IsPETase, a Type IIb enzyme, has been modified by various groups as a promising enzyme because of its high PET hydrolysis activity even at moderate temperatures.[18] On the other hand, PET-degrading enzymes derived from lipases, which are classified as Type IIa, have not been well studied. PET2,[19] discovered as lipase LipIAF5-2 in a metagenomic

Received: June 12, 2024
Revised: July 12, 2024
Accepted: July 15, 2024
Published: July 26, 2024

library of gelatinolytic reactors,[20] is one of the best studied enzymes of Type IIa.

Although its basic structure is the same as that of lipases and esterases, the Trp185 residue of IsPETase is conserved among PET hydrolyzing enzymes and has been thought to enhance PET hydrolyzing activity.[21] The role of Trp 185 has been one of the main subjects of PET hydrolase. There were published papers proposing conformational changes in Trp185 and its involvement in the acylation step.[22] It has also been proposed that conformational variations in Trp185 residues are involved in product release.[23] In addition, it has been proposed that the wobbling of Trp assists the substrate binding and product release.[24] Recently, a computational-analysis paper on the reaction mechanism of IsPETase reported that Trp185 may be involved in the entire reaction cycle.[25] In this paper Trp185 showed two major conformations, with $C-C_\alpha-C_\beta-C_\gamma$ dihedral angles (χ_{1C}) of −60° and +60°. In the former state, the Trp185 side-chain aromatic ring interacts with the aromatic ring of the PET molecular chain in an edge-to-face $\pi-\pi$ interaction during the acylation step. In the latter state, it is postulated that the interaction occurs in an edge-to-face $\pi-\pi$ interaction during the acylation step and in a parallel-displaced $\pi-\pi$ interaction during the deacylation step. The conformation of Trp185 with χ_{1C} = +60° is favorable for both acylation and deacylation steps, while the conformation of χ_{1C} = −60° can contribute to only the acylation step. As experimental results, IsPETase S214H mutant (S185H in the reference) showed lower activity than WT against PET.[23] They reasoned that the steric hindrance caused by the mutation made it difficult for Trp185 to take the conformation χ_{1C} = +60°. In Type I cutinases, the amino acid residue corresponding to the Ser214 of IsPETase is histidine and the orientation of tryptophan is similar to the IsPETase S214H mutant. The combination of His to Ser and Phe to Ile mutations on cutinases increased the PET hydrolysis activity at the expense of heat resistance.[21] The PET2-7M,[26] which is the surface charge modified thermostable mutant of PET2, has His229 and same tryptophan orientation with cutinases.

The depolymerization of PET using enzymes is an area that is attracting attention as an industrial application of enzymes such as food production, paper manufacturing, dairy farming, and environmental remediation.[27] Usually for this purpose, modification of enzymes by rational design[28] or directed evolution[29] is essential to maximize enzyme efficiency. Many methods for activity detection of PET hydrolases are proposed;[30] a simple and accurate activity evaluation system is essential for the analysis of a large number of candidate mutants. In the analysis of PET hydrolases, the substrate PET is insoluble, and the products need to be separated for analysis. Since terephthalic acid, the solubilized product, absorbs in the ultraviolet region, the activity can be quantified from its absorbance change if the enzyme was purified and separated from the medium.[31] But it is very difficult to purify enzymes one by one for rapid activity screening. To measure the activity of crude enzymes, chemosynthesis of soluble fluorescent substrates that mimic PET is needed,[32] and this also requires time to develop the substrates and to verify whether the degradation activity of the model substrate really correlates with that of PET.[33] One potential solution is to utilize the fact that PET is an insoluble substrate for the detection of degradation as an indicator of a decrease in turbidity. Wei et al. prepared agarose beads containing PET nanoparticles and measured the activity of TfCut2.[34] Recently, they developed an insoluble model substrate and immobilized it in polyacrylamide gel beads.[35] They achieved kinetic analysis of TfCa using that substrate.

In this study, a rapid and straightforward method was devised to assess the activity and thermostability of PET-degrading enzymes utilizing PET suspensions. To reduce the cost of substrate preparation for screening, we studied and simplified the condition for PET suspension preparation. Since activity is measured by the reduction in turbidity of the suspension, multiple samples can be evaluated simultaneously, provided a plate reader is available. No purification of the enzyme is required, and the process is straightforward. The method was validated by screening highly active mutants from the PET2-7M-H229X-F233X mutant library (X indicates 20 random amino acids) and evaluating the thermostability using the developed method. The conformation of Trp199 was analyzed to explain the reason for activity improvement in the obtained mutant.

RESULTS

PET Degradation Activity Measurement Based on Turbidity. The initial concentration of PET in 1,1,,3,3,3-hexafluoro-2-propanol was very important. The reduction in the carryover of HFIP to only 1% in a reaction mixture with a final concentration of 0.5 mg mL^{-1} of PET was achieved when a 50 mg mL^{-1} PET solution was used. Absorbance at 595 nm showed liner correlation with PET concentrations in the range 0 to 1 mg mL^{-1} (Figure S1). The PET suspension was sensitive to the ion concentration. The suspension was stable until 50 mM of sodium phosphate buffer, but it aggregated in 100 mM of buffer (Figure S2). The 1 mg mL^{-1} and 0.5 mg mL^{-1} of PET was degraded with the 1 μM of PET2-7M in 50 mM sodium-phosphate buffer pH 7 at 50 °C (Figure 1A). The absorbance of the reaction mixture with 0.5 mg mL^{-1} PET and

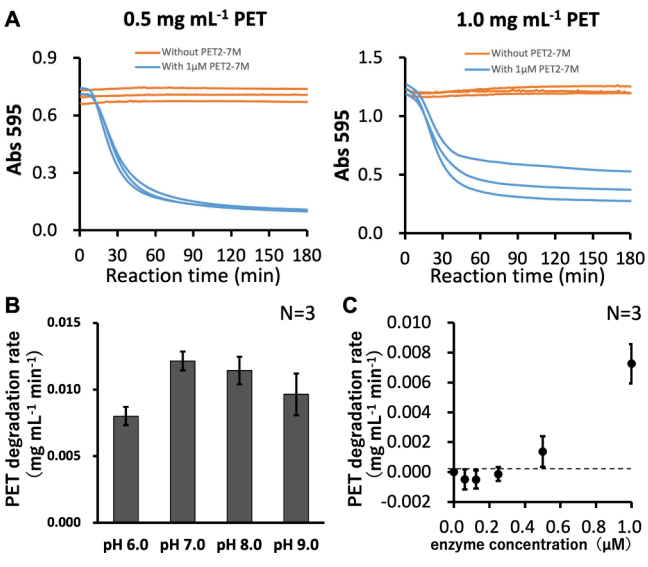

Figure 1. Optimization of conditions for activity screening by turbidity. (A) 0.5 or 1.0 mg mL^{-1} of PET was mixed with 1 μM PET2-7M in 50 mM sodium phosphate pH 7.0 at 50 °C. (B) Degradation rate of 0.5 mg mL^{-1} of PET by 1 μM PET2-7M was compared in 50 mM sodium phosphate pH 6.0, 7.0, Tris-HCl pH 8.0, and glycine-NaOH pH 9.0. (C) Degradation rates of 0.5 mg mL^{-1} of PET by 0.0625 μM to 1 μM PET2-7M were compared in 50 mM sodium phosphate pH 7.0.

https://doi.org/10.1021/acsomega.4c05488
ACS Omega 2024, 9, 34151−34160

PET2-7M was decreased during incubation, but the absorbance of PET without enzyme maintained a constant absorbance. The soluble product concentrations in reaction mixtures were quantified by HPLC (Figure S3). As the value of Abs595 decreased, a linear increase in product concentration was observed in the region used to calculate the degradation rate. These results clearly showed that the PET suspension was solubilized by PET2-7M, and the reaction mixture became clear. When we increase the concentration of PET in the reaction mixture to 1 mg mL^{-1}, the absorbances at 595 nm were decreased with enzyme, but degradation curves did not converge compared to that of 0.5 mg mL^{-1} PET. In addition, when we used the culture medium instead of the purified enzyme, the 1.0 mg mL^{-1} PET showed an increase of absorbance due to the aggregation of PET (Figure S4). Therefore, the activity measurement was done with a 0.5 mg mL^{-1} PET suspension.

The degradation activity of PET hydrolase using turbidity was compared at different pH (Figure 1B). The absorbances at 595 nm of PET without enzyme were almost constant among pH 6 to 9, and the PET particles did not aggregate in this range of pH and concentrations of buffers. The velocity of turbidity decrease by 1.0 μM PET2-7M at pH 7 and 50 °C ($(1.2 \pm 0.1) \times 10^{-2}$ mg mL^{-1} min^{-1}) was the highest, and the velocities were decreased in higher or lower pH. The lower detection limit of concentration of PET2-7M was 0.5 μM, and the activity value was $(1.4 \pm 0.1) \times 10^{-3}$ mg mL^{-1} min^{-1} (Figure 1C). At lower than 0.5 μM enzyme, noise and partial aggregation caused a temporal increase of turbidity and was detected as a negative degradation rate of PET. Therefore, we tried to use 1.0 μM enzyme ($(7.3 \pm 1.3) \times 10^{-3}$ mg mL^{-1} min^{-1}) to stabilize the activity measurement.

Direct Activity Measurement from Medium and Optimization of Cultivation Conditions. We compared the two types of cultivation with *E. coli* transformed by the plasmid encoding PET2-7M. One was 24 h cultivation from colonies to grow the cells and simultaneous 24 h cultivation with IPTG to produce the enzymes (without preculture). Colonies were inoculated in 1 mL of medium, and enzyme production was induced by IPTG after 9 h of incubation. The other method was with preculture. A 100 μL amount of medium after 24 h of cultivation from colonies was inoculated to the 900 μL of fresh medium. After 2 h of cultivation, IPTG was added to produce the enzyme and further cultivated for 22 h. The activity of the sample without preculture medium ($(6.7 \pm 1.0) \times 10^{-3}$ mg mL^{-1} min^{-1}) was higher than that with preculture medium ($(4.3 \pm 1.0) \times 10^{-3}$ mg mL^{-1} min^{-1}) (Figure 2A). The protein concentration without preculture medium (1.3 ± 0.1 mg mL^{-1}) was 3 times higher than that with preculture medium (0.42 ± 0.06 mg mL^{-1}) (Figure 2B). Therefore, the specific activity with preculture medium ($(1.0 \pm 0.2) \times 10^{-2}$ min^{-1}) was 2 times higher than that without preculture medium ($(5.1 \pm 0.2) \times 10^{-3}$ min^{-1}) (Figure 2C). The SDS-PAGE of the two samples showed a clear band of PET2-7M at 28 kDa (Figure 2D). The intensity of the PET2-7M band without preculture medium was stronger than that with preculture medium, but the other bands of contaminants were also stronger. These bands are proteins from *E. coli* because they did not appear in the medium without *E. coli*. The amount of medium for activity measurement was also evaluated (Figure S5). A 10 μL amount of culture medium showed the activity of $(6.5 \pm 0.1) \times 10^{-3}$ mg mL^{-1} min^{-1}, and the value was enough to be detected. When we mixed 25 μL of culture medium in the reaction mixture, the PET degrading rate was $(8.1 \pm 1.3) \times 10^{-3}$ mg mL^{-1} min^{-1} and very close to the activity with 1 μM purified PET2-7M. Therefore, we used 25 μL of culture medium for activity screening of mutants.

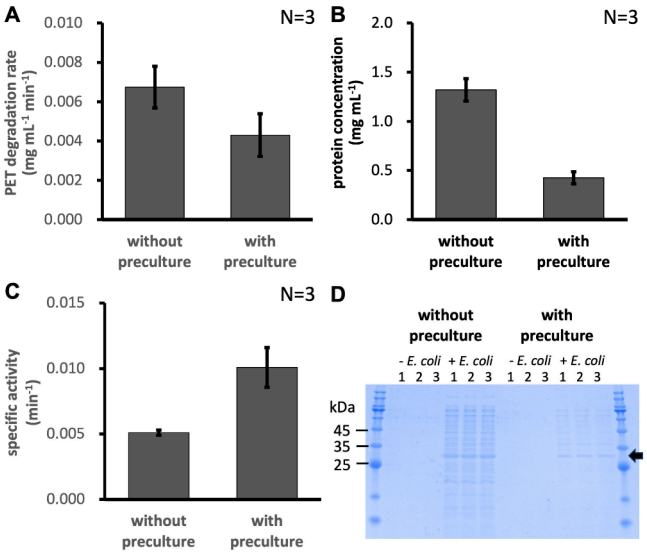

Figure 2. Optimization of culture conditions for production of PET2-7M. (A) PET degradation rates with supernatant of medium with and without preculture. (B) Protein concentrations in supernatant of medium with and without preculture. (C) Specific activity of PET degradation of medium with and without preculture. (D) SDS-PAGE of medium with and without preculture.

Screening of High-Activity Mutant. To verify the activity screening with turbidity, we tried to screen the PET2-7M-H229X-F233X mutant library. The samples with preculture medium of colonies were mixed with a PET suspension, and PET degradation activities were measured at 50 °C. Theoretical combinations of amino acids were 399, and we screened 720 colonies of the mutants (Figure 3A). The 24 colonies of PET2-7M were also cultivated as a control, and the average value was plotted with standard deviations of activity and protein concentration.

Thirty-five colonies showed a more than 4.0×10^{-3} mg mL^{-1} min^{-1} PET degrading rate (except for two colonies) and 2 times higher specific activity against PET2-7M ($(2.2 \pm 0.5) \times 10^{-2}$ min^{-1}). These were purified, and the mutations were verified by sequencing (orange squares and blue diamonds in Figure 3A). The all-amino-acid combinations of variants are shown in Figure S6.

Sequence-confirmed mutants were classified into three groups. One is the most likely group with a PET degradation rate higher than 9.0×10^{-3} mg mL^{-1} min^{-1} and a protein concentration higher than 5.0×10^{-2} mg mL^{-1}. Twelve mutants were included in this group, but three colonies were H229V-F233Y, and a further two colonies were H229V-F233M or H229I-F233M, giving a total of 8 mutant types. The second group, with moderate protein concentration and PET degradation rate, contained 19 colonies. However, it was located in the top left of the population, and its specific activity around the protein was estimated to be higher than that of PET2-7M. Triplication of H229L-F233L and H229V-F233L and duplications of H229R-F233L gave 14 mutant types. The last group consisted of four mutants with very low protein concentrations, H229W-F233F, H229R-F233V, H229L-F233S, and H229G-F233A.

https://doi.org/10.1021/acsomega.4c05488
ACS Omega 2024, 9, 34151−34160

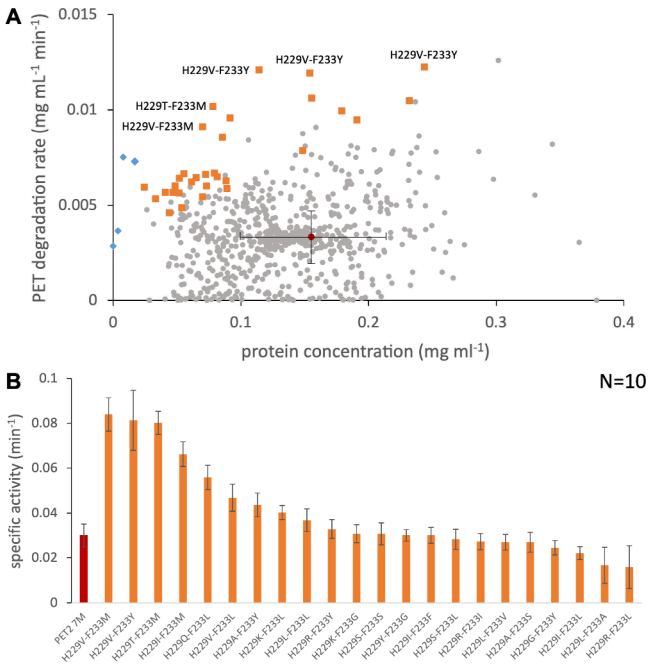

Figure 3. Screening of high-activity mutants. (A) PET degradation activities and protein concentrations of 720 colonies of variants were plotted. Orange squares are sequenced colonies as candidates for higher activity variants. Blue diamonds are sequenced as variants with high activity but low production. The average and standard deviation values of 24 colonies of PET2-7M are plotted as a red circle. (B) Specific activities of PET2-7M and 22 candidates. Ten colonies were cultivated individually, and their activities and protein concentrations were analyzed.

To verify the activities of variants, the purified plasmids of 22 candidates for high activity variants were re-transformed in *E. coli*, and 10 different colonies were inoculated in the medium (Figure 3B). The specific activity of PET2-7M was $(3.0 \pm 0.5) \times 10^{-2}$ min^{-1}. The three most active mutants were H229V-F233M, H229V-F233Y, and H229T-F233M, with activities of $(8.4 \pm 0.7) \times 10^{-2}$ min^{-1}, $(8.1 \pm 1.3) \times 10^{-2}$ min^{-1}, and $(8.0 \pm 0.5) \times 10^{-2}$ min^{-1}, respectively. These values were more than 2.5 times higher than the activity of PET2-7M. The fourth most active mutant was H229I-F233M, with $(6.6 \pm 0.6) \times 10^{-2}$ min^{-1}, which was about twice as active as PET2-7M, suggesting that the top three mutants were candidates for highly active mutants. The 13th H229Y-F233G had an activity of $(3.0 \pm 0.3) \times 10^{-2}$ min^{-1}, close to that of PET2-7M. Subsequent mutants were found to have lower specific activity than PET2-7M.

The mutations tended to be at His229 with small, branched side chains such as Val and Thr, which contributed to the increased activity. Large amino acids such as Tyr, Arg, and Lys and too small amino acids such as Ala and Gly tended to be less active, while Ser, the same as in IsPETase, was not found in the mutants more active than PET2-7M. The F233 mutation was Met in the four active mutants. F233Y was the second most active mutant, but the same mutation was present in the seventh, 10th, and 19th mutants. While in IsPETase it was Ile, the F233I mutation does not increase or decrease the activity of PET2-7M.

Thermostability Screening. The reaction temperature for activity screening was limited by the temperature control ability of the micro plate reader. In this paper we used 50 °C for activity screening; therefore we could not evaluate the thermostabilities of variants at a higher temperature than 50 °C in the normal screening. Therefore, for the thermostability screening, we pretreated the collected medium using a thermal cycler with a temperature gradient of 50 to 75 °C for 1 h, and the remaining activities were measured at 50 °C by the turbidity screening method (Figure S7). Using our methods, 12 mutants and the template PET2-7M were evaluated in triplicate at once with a 384-well plate.

PET2-7M showed almost constant activity until 70 °C, and the activity was lost after 1 h of heating at 75 °C. All 12 mutants demonstrated a lower thermostability than PET2-7M (Figure S7). This result might be due to the high flexibility of Trp199 as reported in the other PET hydrolases.[36,37] The best three mutants, H229T-F233M, H229V-F233Y, and H229V-F233M, showed higher specific activities than the other mutants after heat treatment at 59 °C (Figure 4). Their

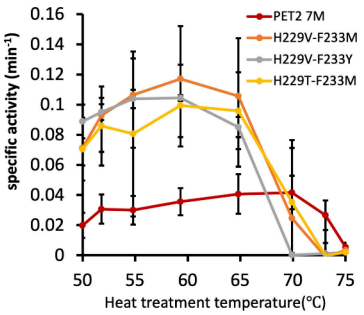

Figure 4. Thermostability screening of PET2-7M and the best three variants. A 100 μL amount of culture mediums was heated at 50 to 75 °C for 1 h, and retained activities were analyzed at 50 °C. Activities were measured three times.

activities were also higher than the others after 65 °C treatment, but the values were smaller than the 59 °C treatment. These results indicated that the three mutants gradually denatured at more than 60 °C. After 1 h of incubation at 70 °C, H229T-F233M and H229V-F233M mutants retained some activities, but other mutants completely lost their activities.

PET Film Degradation Activity Measurement. The H229T-F233M, H229V-F233Y, and H229V-F233M mutants, which showed more than 2 times higher activity than PET2-7M after 59 °C incubation, were produced in large-scale cultivation and purified to evaluate the activity against a film substrate. The PET film-degrading activities of the three mutants were compared with the template PET2-7M. The degradation activities were measured at both pH 7 and pH 8. As in previous papers, PET2-7M showed higher PET film-degrading activity at pH 8 than at pH 7. The H229V-F233M and H229T-F233M mutants also showed 1.1- and 1.8-fold higher PET film-degrading activity at pH 8 than at pH 7, respectively (Figure 5A and B). In contrast, the H229V-F233Y mutant exhibited a 50% reduction in activity at pH 8 relative to pH 7. The highest activity among the mutants was observed in the H229T-F233M mutant at pH 8, which was 5.7-fold higher than PET2-7M.

The most active mutant, H229T-F233M, was compared with PET2-7M for degradation activity over long periods of time (Figure 5C). Between the initial speed and 24 h at the end of the reaction, the mutant consistently produced more product than PET2-7M. The mutant produced 1205 μM total

https://doi.org/10.1021/acsomega.4c05488
ACS Omega 2024, 9, 34151−34160

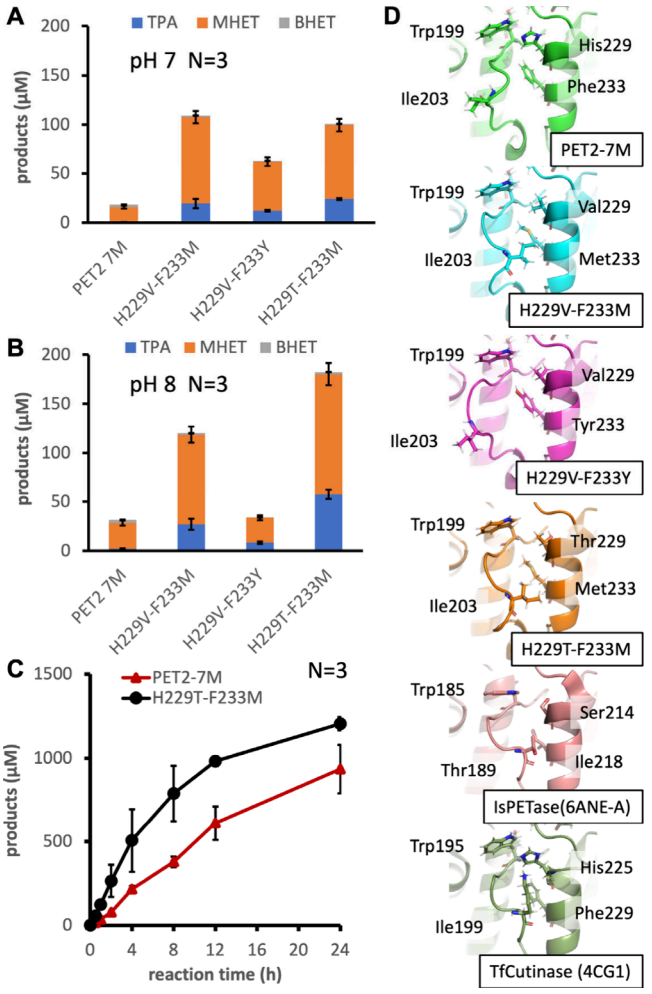

Figure 5. PET film degradation activities and predicted structures of variants. (A) PET film degradation by 100 nM enzymes at 60 °C for 1 h in 50 mM sodium phosphate pH 7.0. (B) PET film degradation by 100 nM enzymes at 60 °C for 1 h in 50 mM sodium phosphate pH 8.0. (C) Degradation of PET film by PET2-7M and H229T-F233M mutants at 60 °C in 50 mM sodium phosphate pH 7.0. (D) Comparison of predicted structures by Alphafold2. The IsPETase (6ANE chainA) and cutinase from *Thermobifida fusca* (4CG1).

product in 24 h of reaction. The difference in product concentration decreased with time, suggesting that the mutant degraded the PET molecular chain at an increased rate, but did not increase the area available for degradation.

The structures of variants were predicted by Alphafold2 and compared with PET2-7M, IsPETase, and TfCutinase (Figure 5D). The predicted structure of PET2-7M was completely the same as the X-ray crystal structure (PDB ID: 7EC8). Focusing on the orientation of Trp199, PET2-7M and the mutant had almost the same angle as TfCutinase and was different from IsPETase. On the other hand, the loop structure in which Trp199 was located was different between PET2-7M and the mutant. The loops of H229V-F233M and H229T-F233M, which were more active than PET2-7M, were close to IsPETase. The loop of H229V-F233Y was bent and was exposed to solvent.

MD Simulation of PET2-7M and H229T-F233M. To reveal the reason for the better activity of H229T-F233M than PET2-7M, we performed molecular dynamics simulation for 100 ns. The main chain dihedral angles of Trp199 were analyzed and compared between the two enzymes. The distribution of the plots differed for H229T-F233M and PET2-7M, reflecting the differing structure of the loop in the predicted conformation. The mean values and standard deviations of phi and psi for each enzyme were analyzed, with the results showing phi = −133.0 ± 13.6° and psi = 141.1 ± 8.4° for H229T-F233M and phi = −105.1 ± 19.0° and psi = 128.9 ± 11.7° for PET2-7M (Figure 6A). Furthermore, the temporal variation of the side-chain dihedral angle (chi1) of Trp199 was analyzed. In H229T-F233M, the angle oscillated at 59.2 ± 8.4°, whereas in PET2-7M, it was 65.7 ± 7.1°, indicating a difference in the angle that could be stably taken (Figure 6B).

The frames closest to the mean structure of H229T-F233M and PET2-7M, respectively, were extracted and compared to the structure of IsPETase (Figure 6C). The average structure of H229T-F233M (orange) was very similar to the crystal structure of IsPETase (pink 6ANE chain A), not only the angle of Trp199, but also the loop structure. In contrast, the angle of Trp199 was very different in PET2-7M (green), and the loop structure was also different from IsPETase.

DISCUSSION

PET suspensions created by direct regeneration from HFIP solution to water are indeed prone to agglomeration and difficult to handle. However, we found that PET suspensions of 0.5 mg mL^{-1} in the reaction mixture did not aggregate and that the decrease in turbidity due to enzymatic degradation was sufficient to be observed. It was also found that an ionic strength of about 50 mM was appropriate for the buffer, since raising the buffer ionic strength too high can cause aggregation. The high salt concentration is thought to cause aggregation by canceling the electrification repulsion between PET particles. PET at 0.5 mg mL^{-1} yields about 2.4 mM terephthalic acid and ethylene glycol upon complete degradation; a buffer strength of 50 mM is sufficiently high to provide buffer capacity. In addition, 1.0 mg mL^{-1} PET was aggregated by adding 10 μL of medium (Figure S4). Wei et al. used 0.5 M Tris-HCl pH 8.0 for the activity measurement with a PET suspension immobilized in agarose beads,[34] and Matheus et al. used 0.2 M Tris-HCl pH 8.0 for the activity measurement with a PET suspension immobilized in polyacrylamide beads.[35] If the reaction needs to be carried out under higher ionic strength conditions, stabilization methods such as theirs are necessary.

The production of PET2-7M was found to be effective in increasing enzyme purity and specific activity through the process of preculturing (Figure 2C). The mechanism by which PET2-7M is secreted from the periplasmic region of *E. coli* into the culture medium remains unknown. However, given the detection of a large number of protein bands under the condition of no preculture (Figure 2D), it is possible that this process is accompanied by lysis of a part of the outer membrane of *E. coli*.[38] In the case of cutinases, secretion of enzyme into culture medium induced by the limited phospholipid hydrolysis was reported.[39,40] Additionally, the detection of IsPETase with pelB signal in the culture medium was also reported.[41] It is possible that PET hydrolase leaks into the medium since even larger chitin hydrolases (~100 kDa) have been reported to be secreted into the culture medium.[42]

In the PET2-7M-H229X-F233X screening, the majority of mutants exhibited activity within the standard deviation of PET2-7M (Figure 3A). Of the 399 potential mutant combinations, 12 variants exhibited greater activity than

https://doi.org/10.1021/acsomega.4c05488
ACS Omega 2024, 9, 34151−34160

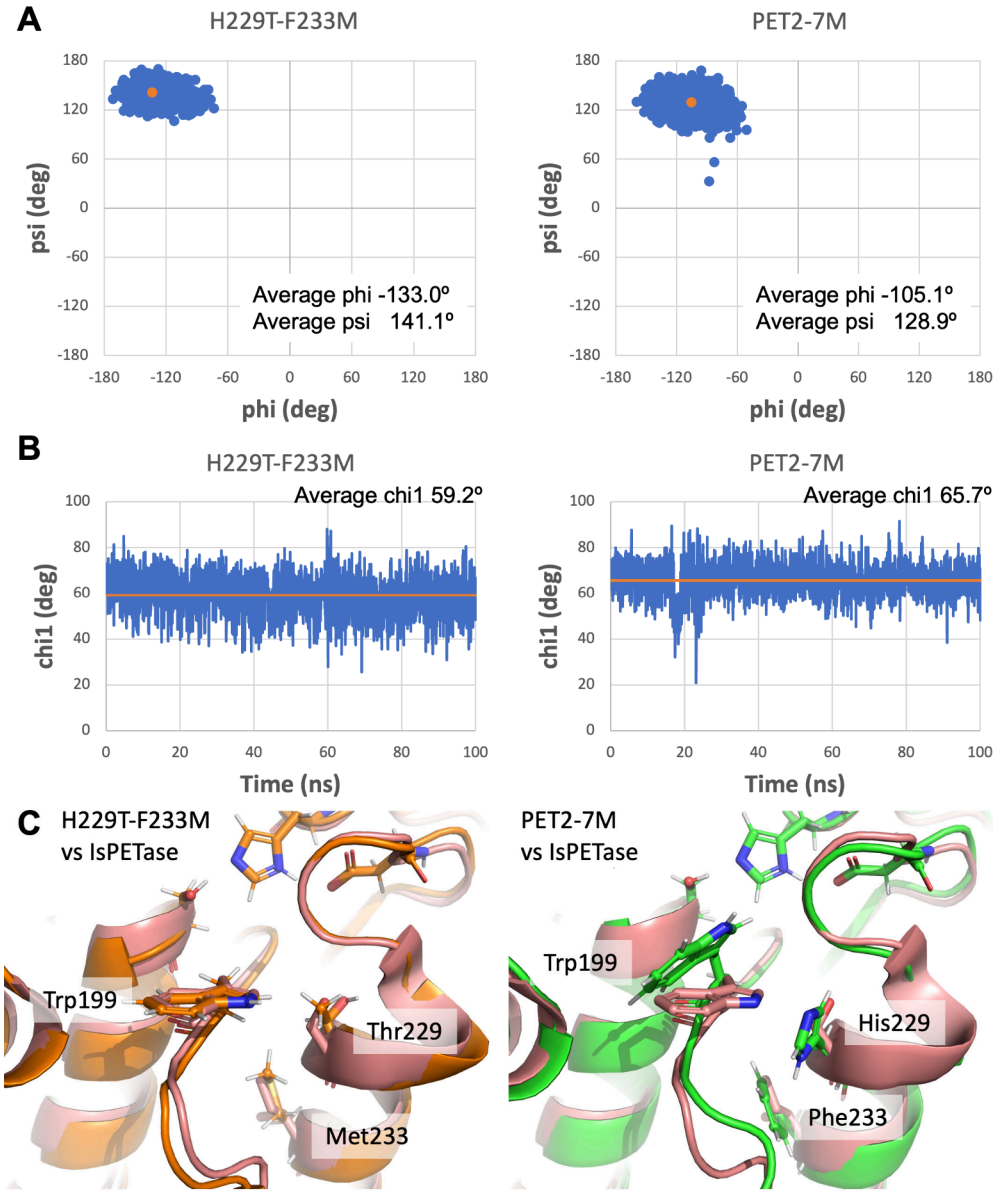

Figure 6. MD simulations of PET2-7M and H229T-F233M variant. (A) Plots of dihedral angles (phi and psi) of Trp199 during a 100 ns simulation. The average of the two angles were plotted in orange. (B) Temporal fluctuations of Chi1 during simulation. The average angles are shown by orange lines. (C) The average structure of H229T-F233M and PET2-7M. The IsPETase structure is shown in pink (6ANE chain A).

PET2-7M, resulting in an improvement rate of 3% (Figure 3B). The 12 variants showed improved activities, but lower thermostability than the template enzyme. This may be because their flexibilities of Trp199 are higher than the PET2-7M (Figure 5D). Given H229G-F233A and H229W(-F233) mutants showed lower enzyme concentration, too much larger or smaller residues are not suitable for these positions. Therefore, we need to have a balance of thermostability and activity at these positions. The PET hydrolase found in metagenomic library PHL7 was point mutated at these two positions. PHL7-H185S and PHL7-F189I mutants showed 11.5 and 7 °C lower T_m than PHL7 WT.[36] The metagenomic library-derived BhrPEase,[43] which has 94% sequence identity with LCC and the template of TurboPETase,[37] has been introduced with the H218S-F222I mutation. BhrPETase M2 (H218S-F222I mutant) showed 2.5 times higher activity than BhrPETase WT, but the BhrPETase M2 variant exhibited a melting temperature of 85 °C, which was 11 °C lower than that of the wild-type enzyme. We screened the degradation activity of our mutant library at 50 °C. Therefore, we could not find the PET2-7M-H229S-F233I mutant in the pool of high-activity mutants.

The top 3 mutants (H229V-F233M, H229V-F233Y, and H229T-F233M) in turbidity measurement showed better activity against PET film at pH 7. But the activity of H229V-F233Y was decreased at pH 8. Even if the pK_a of the tyrosine side chain is around 10, almost one percent of the tyrosine is deprotonated at pH 8. A small amount of deprotonation might be enough to reduce the activity, if a minus charge makes the core structure unstable. In the sequenced mutants, all of them have an uncharged and hydrophilic residue in the F233X position. These results support this hypothesis. The difference of the H229V-F233M and H229T-F233M is the methyl or hydroxyl group of the side chain. The α helix, H229T-F233M located, is capped by a proline residue, and the carboxyl of Ala197 makes a hydrogen bond with the side chain of Thr229

https://doi.org/10.1021/acsomega.4c05488
ACS Omega 2024, 9, 34151−34160

(Figure 5D). This interaction of H229T-F233M is believed to result in a higher heat resistance than that observed with H229V-F233M (Figure 4).

The PET2-7M-H229T-F233M variant exhibited enhanced activity relative to the PET2-7M in turbidity measurement and PET film degradation. However, these two mutated residues do not directly interact with the PET chain. The most probable reason for the activity improvement is the difference of the flexibility of Trp199 of PET2 as Chen et al. suggested in IsPETase and other PET hydrolases.[21] In the Alphafold2 prediction, the most notable difference between the two enzymes is the structural composition of the loop region, where the Trp199 residue is located (Figure 5D). In the molecular dynamics simulation, the structure of the loop and the chi1 angle of Trp199 of the PET2-7M-H229T-F233M variant are similar to those of IsPETase (Figure 6C).

Mutation of the same amino acid as other cutinase or PETase mutants is not always optimal because the appropriate amino acid residue depends on the status of the surrounding amino acids. The F233M mutation found in this paper is the appropriate mutation for PET2 and differs from previously reported mutants of IsPETase or cutinases. DuraPETase[44] has the S214H mutation and HotPETase[45] has the S214Y mutation, respectively. These two mutants have Ile218 and Thr189 residues and have a space for Tyr or His without affecting the Trp185 orientation.

H229-F233 of PET2 is conserved in both cutinase (Type I) and Type IIa enzymes. But the loops with Trp199 have sequence differences. Cutinase has solvent-oriented Lys residues (Lys194 at LCC and Lys199 at TfCut2), so there is space for Phe at the same position as Phe233 of PET2. In addition, the activity of LCC-ICCG was increased by H218Y mutation.[46] On the other hand, PET2-7M has a different loop structure because the length is one amino acid longer than cutinase, the side chain of Ile203 interferes with Phe233, and the angle of Trp199 is unsuitable for PET degradation. The F233M mutation in PET2 creates space on the Ile side chain, folding a stable helix that allows the formation of a loop structure similar to that of IsPETase. The H229T mutation of PET2 was recently reported as an S214T mutation of IsPETase by Joho Y. et al.[47] They reported that the S214T mutation increased the activity of IsPETase by 12%. The serine to threonine mutation is effective for Type IIa and IIb enzymes. This mutation is likely to be effective in cutinases, because the proline residues making a hydrogen bond with Ser/Thr are conserved in all types of PET hydrolases.

Recently, computational designing of PET hydrolases has been reported, resulting in significant improvements in performance.[37,44,48] The activity screening method using PET suspensions reported in this paper is highly useful for the validation of predicted results. Furthermore, the 96-well and 384-well plates allow all reagents to be handled in solution and measured with a microplate reader, rendering it compatible with automated pipetting robots. In conjunction with a colony picker, the system can be nearly entirely automated, which will facilitate the development of more highly functional enzymes.

METHODS

Enzyme Production and Purification. *E. coli* C41 (DE3) was transformed with the pET27b plasmid coding PET2-7M (R47C-G89C-F105R-E110K-S156P-G180A-T297P) or three variant genes and incubated in SOC culture medium at 37 °C for 1 h. Then, it was incubated overnight on a LB plate containing 50 μg/mL kanamycin at 37 °C. A colony was inoculated into two 2 L flasks with 700 mL of super broth medium (2.5% tryptone, 1.5% yeast extract, 0.5% sodium chloride) containing 25 μgmL^{-1} kanamycin and incubated at 37 °C and 130 rpm for 3.5 h. Then 700 μL of 1 M IPTG was added to each flask and incubated overnight at 16 °C and 130 rpm. The *E. coli* culture medium was centrifuged at 3100*g* for 15 min, and cells were harvested. Cells were stored in a freezer at −80 °C until use.

Cells were suspended in 50 mM sodium phosphate pH 7.0 containing 100 mM sodium chloride at a concentration of 10 g/100 mL and sonicated on ice for 20 min. The supernatant was collected after centrifuging at 20000*g* and loaded in the Ni-NTA agarose (CV = 5 mL). The column was washed with 50 mL of buffer and further washed with 50 mL of buffer containing 50 mM imidazole; the target enzyme was eluted with buffer containing 100 mM imidazole and concentrated using VIVAspin20 (MWCO 10K). Imidazole was removed with NAP10 columns. The enzymes were mixed with 100 μL of 3 mg/mL TEV protease and incubated overnight at 16 °C. The enzymes were passed through Ni-NTA agarose (CV = 1 mL) and eluted with buffer. Enzymes were concentrated using VIVAspin20 (MWCO 10K) and loaded in Superdex75 Increase. The purified enzyme was stored in glass vials at 4 °C.

Preparation of PET Suspension and Standard Curve. A 50 mg amount of amorphous PET film (Goodfellow, code ES301445) was dissolved in 1 mL of 1,1,1,3,3,3-hexafluoro-2-propanol, and 50 mg mL^{-1} PET solution was prepared. Then 0, 0.125, 0.25, 0.5, 1.0, 2.0, and 3.0 mg mL^{-1} PET suspensions containing 50 mM sodium phosphate pH 7.0 were prepared, and the absorbance at 595 nm was measured with a microplate reader. Calibration curves were prepared, and the relationship between PET concentration and absorbance was examined. A 225 μL amount of a 50 mg/mL PET solution was added in 1275 μL of Milli-Q water to prepare a theoretically 7.5 mg mL^{-1} PET suspension for activity screening. The concentration of PET was calibrated using a standard curve before use.

Effect of Buffer Concentration. A 7.5 mg/mL PET suspension, 1 M sodium phosphate pH 7.0, and Milli-Q water were mixed. The final PET concentration was 1.0 mg mL^{-1}, and sodium phosphate buffer concentrations were changed from 0 to 100 mM. The PET suspensions were incubated at room temperature for 1 min, and formation of aggregations was observed.

Effect of PET Concentration. A 10 μL amount of purified 10 μM PET2-7M, 13.2 μL of 7.5 mg mL^{-1} or 3.25 mg mL^{-1} PET suspension, 5 μL of 1 M buffer, and 71.8 μL of Milli-Q water were mixed on the 384-well plate. Absorbance at 595 nm (Abs 595) was measured every minute for a total of 3 h at 50 °C with a microplate reader. To measure the concentrations of products in the reaction mixture, 1 μM PET2-7M was mixed with 0.5 mg mL^{-1} PET suspension in 50 mM sodium phosphate pH 0. The reaction mixtures were collected when the decrease of Abs 595 was 0.038, 0.161, and 0.315. The reaction mixtures were centrifuged at 20000*g* for 5 min, and the supernatants were injected to HPLC. The activity assay was performed in triplicate. To check the effect of medium, the supernatant of the *E. coli* culture medium harvested was used instead of purified PET2-7M.

pH Dependence. A 10 μL amount of 10 μM PET2-7M enzyme solution, 6.6 μL of 7.5 mg mL^{-1} PET suspension, 5 μL

https://doi.org/10.1021/acsomega.4c05488
ACS Omega 2024, 9, 34151−34160

of 1 M buffer, and 78.4 μL of Milli-Q water were mixed in the 384-well plate. Absorbance at 595 nm (Abs 595) was measured every minute for a total of 3 h at 50 °C with a microplate reader. The tested buffers were sodium phosphate pH 6.0 and pH 7.0, Tris-HCl pH 8.0, and glycine−NaOH pH 9.0. The activity assay was performed in triplicate.

The absorbance at 595 nm was converted to the PET concentration using the coefficient 1.468 $(mg/mL)^{-1}$ obtained from the standard curve of the PET suspension (Figure S1). PET degradation rate per minute was calculated as an average of the decrease during 10 min, and the values were calculated throughout the entire reaction time. The maximum value of PET degradation rate per minute was used as the enzyme activity value.

Lower Limit of Enzyme Concentration for Activity Detection. A 10 μL amount of 10, 5, 2.5, 1.25, 0.625, and 0 μM PET2-7M, 6.6 μL of 7.5 mg mL^{-1} PET suspension, 5 μL of 1 M sodium phosphate pH 7.0, and 78.4 μL of Milli-Q water were mixed, and absorbance at 595 nm was measured every minute for a total of 3 h at 50 °C. The activity values were calculated by the same method.

Enzyme Production for Activity Screening. PET2-7M on the pET27b plasmid was amplified with mixed primer (NNK) at positions H229 and F233 using KOD One PCR master mix. The amplified genes were separated by gel electrophoresis and extracted and purified by Wizard SV gel and PCR clean-up system. The purified gene was ligated by NEBuilder HiFi DNA assembly master mix, and the variant library was constructed. *E. coli* Tuner (DE3) was transformed with the pET27b plasmid inserted PET2-7M or variant gene library and incubated in SOC culture medium at 37 °C for 1 h. Then, it was incubated overnight on an LB plate containing 50 μgmL^{-1} kanamycin at 37 °C. The colony was inoculated into 1 mL of super broth medium (2.5% tryptone, 1.5% yeast extract, 0.5% sodium chloride) containing 50 μg mL^{-1} kanamycin in 96-well plates and incubated at 37 °C and 1000 rpm.

In the case without preculture condition, 10 μL of 100 mM IPTG was added to each well of the plates after 9 h of incubation and further incubated overnight at 37 °C at 1000 rpm. For the sample with preculture condition, 100 μL of medium after 24 h of cultivation was inoculated in the fresh 900 μL medium and cultivated for 2 h. A 10 μL amount of 100 mM IPTG was added to each well of the plates and further incubated overnight at 37 °C at 1000 rpm.

The *E. coli* culture medium in 96-well plates was centrifuged at 3100*g* for 5 min, and 500 μL of supernatant was harvested.

Enzyme Activity Screening. The supernatant of the *E. coli* culture medium harvested was used as an enzyme solution. A 10 μL amount of PET2-7M or variant enzyme solution, 6.6 μL of 7.5 mg mL^{-1} PET suspension, 5 μL of 1 M buffer, and 78.4 μL of Milli-Q water were mixed in the 384-well plate. Abs 595 was measured every minute for a total of 3 h at 50 °C with a microplate reader. The activity values were calculated by the same method. Enzyme solution volume was changed to 10, 25, and 50 μL. The activity assay was performed on 10 samples per condition.

The protein concentrations in the culture medium were determined by a TaKaRa Bradford protein assay kit. A 2 μL amount of culture medium and 100 μL of Bradford dye reagent were mixed on the 384-well plate, and Abs 595 was measured with a microplate reader. We created a calibration curve using a BSA standard solution and calculated the protein concentrations in the culture medium.

Thermostability Screening. Thirty-five colonies with higher specific activity than PET2-7M were chosen, and plasmid extraction was performed using cells stored at −80 °C by QIAprep Spin miniprep kit. Purified plasmid DNA was analyzed for sequencing by Eurofins Genomics.

High-activity variants were produced using purified plasmids. A 50 μL amount of the *E. coli* culture medium was dispensed into 8 tubes, and thermal treatment was performed using the temperature gradient option of the thermal cycler. The activity assay was performed after heat treatment of the enzyme at 50−75 °C for 1 h. After heat treatment, 25 μL of enzyme solution was mixed with 75 μL of PET suspension (final concentration is 0.5 mg mL^{-1}) containing 50 mM Na-phos pH 7.0 on a 384-well plate. The activity assay was performed in triplicate.

PET Film Degradation. TPA and MHET solutions of 800, 400, 200, 100, 50, 25, 12.5, and 6.25 μM were prepared by diluting a 100 mM TPA solution and 10 mM mono-2-hydroxyethyl terephthalate (MHET) + 20 mM Na-phos pH 8.0 solution, respectively. Bis-2-hydroxyethyl terephthalate (BHET) solutions of 40, 20, 10, 5, and 2.5 μM were prepared by diluting a 400 μM TPA+MHET+BHET solution. Each sample was analyzed by high-performance liquid chromatography (HPLC) to prepare a calibration curve.

Amorphous PET films (Goodfellow (code ES301445)) were punched out into a 5.5 mm diameter circle, washed with 20% ethanol for 1 h with rotation, and dried. One PET disk was placed in a vial; then 10 μL of a 2.5 μM enzyme solution, 12.5 μL of a 1 M Na-phos buffer (pH 7.0 or pH 8.0), and 227.5 μL of Milli-Q water were added. The enzyme was incubated at 60 °C for 1 h. The supernatant was collected and analyzed by HPLC. The reaction solutions without enzyme were used as the control. The activity assay was performed in triplicate.

HPLC was performed using a Kinetex 2.6 μm EVO C18 100 Å LC column (150 × 3.0 mm). The mobile phase was 0.1% formic acid and acetonitrile. Each sample was injected at a volume of 10 μL, and compounds were detected at a wavelength of 240 nm. Product concentrations were calculated using a calibration curve.

In addition, the changes over time of product concentrations were examined. One PET disk was placed in a vial; then 10 μL of a 2.5 μM enzyme solution, 12.5 μL of 1 M Na-phos buffer pH 8.0, and 227.5 μL of Milli-Q water were added. The enzyme was incubated at 60 °C for 0.5, 1, 2, 4, 8, 12, and 24 h. Each sample was analyzed by HPLC, and product concentrations were calculated.

Structure Prediction. The structures of PET2-7M and H229T-F233M, H229V-F233Y, H229V-F233M mutants were predicted using Alphafold2 ver. 2.3.2 with the MGnify data set, May 2023 version. Five models were generated per enzyme, and the best scored structures were relaxed.[49] The predicted structures were visualized and aligned to PET2-7M by Pymol.

Molecular Dynamics Simulation. Predicted structures of PET2-7M and H229T-F233M were used as the initial model, and MD simulations were performed using OpenMM ver. 8.1.1.[50] The data for simulation were prepared using an OpenMM Setup script. The force field applied for proteins was Amber14, and that for water was TIP3P-FB.[51] The water molecules were added around the enzyme with 1 nm padding distance and 0.1 M sodium chloride in cubic boxes. Temperature and pressure were set to 300 K and 1 atm using a Langevin thermostat/barostat. A 10 Å cutoff radius was used for short-range interactions, and particle-mesh Ewald

https://doi.org/10.1021/acsomega.4c05488
ACS Omega 2024, 9, 34151−34160

(PME) was used for long-range electrostatic interactions The systems were minimized for 0.1 ps and equilibrated for 4 ps with dt = 4 fs. The productions were 100 ns, and the distributions of dihedral angles were analyzed using VMD.[52]

■ ASSOCIATED CONTENT

Supporting Information

The Supporting Information is available free of charge at https://pubs.acs.org/doi/10.1021/acsomega.4c05488.

Figures of the standard curve of absorbance and PET suspension concentration, buffer concentration sensitivity of the PET suspension, quantification of products from the PET suspension by HPLC, degradation of 0.5 and 1.0 mg mL^{-1} PET with culture medium, PET degradation activity depending on the volume of culture medium, sequence results of high-activity mutants, results of thermostability screening of 12 mutants (PDF)

■ AUTHOR INFORMATION

Corresponding Author

Akihiko Nakamura − *Department of Applied Life Sciences, Faculty of Agriculture and Research Institute of Green Science and Technology, Shizuoka University, Shizuoka 422-8529, Japan; Shizuoka Institute for the Study of Marine Biology and Chemistry, Shizuoka, Shizuoka 422-8529, Japan; Institute for Molecular Science, National Institutes of Natural Sciences, Okazaki, Aichi 444-8787, Japan;* orcid.org/0000-0003-0409-5759; Email: aki-naka@shizuoka.ac.jp

Authors

Yui Ogura − *Department of Agriculture, Graduate School of Integrated Science and Technology, Shizuoka University, Shizuoka 422-8529, Japan*

Yoshihito Hashino − *Department of Agriculture, Graduate School of Integrated Science and Technology, Shizuoka University, Shizuoka 422-8529, Japan*

Complete contact information is available at: https://pubs.acs.org/10.1021/acsomega.4c05488

Author Contributions

Yui Ogura: Investigation, Formal analysis, Validation, Visualization, Writing−Original draft preparation. Yoshihito Hashino: Formal analysis. Akihiko Nakamura: Conceptualization, Resources, Project administration, Supervision, Visualization, Funding acquisition, Writing−Original draft preparation, Writing−Reviewing, and Editing.

Funding

This study was supported by MEXT Leading Initiative for Excellent Young Researchers Grant Number 201990171, Grants-in-Aid for Scientific Research 24K01990 (to A.N.) from the Ministry of Education, Culture, Sports, Science, and Technology of Japan, and JST FOREST Program (Grant Number JPMJFR210C, Japan).

Notes

The authors declare no competing financial interest.

■ REFERENCES

(1) Nisticò, R. Polyethylene Terephthalate (PET) in the Packaging Industry. *Polym. Test.* **2020**, *90*, 106707.

(2) Lange, J.; Wyser, Y. Recent Innovations in Barrier Technologies for Plastic Packaging—a Review. *Packaging Technology and Science* **2003**, *16*, 149−158.

(3) Geyer, R.; Jambeck, J. R.; Law, K. L. Production, Use, and Fate of All Plastics Ever Made. *Sci. Adv.* **2017**, *3*, No. e1700782.

(4) Muringayil Joseph, T.; Azat, S.; Ahmadi, Z.; Moini Jazani, O.; Esmaeili, A.; Kianfar, E.; Haponiuk, J.; Thomas, S. Polyethylene Terephthalate (PET) Recycling: A Review. *Case Studies in Chemical and Environmental Engineering* **2024**, *9*, 100673.

(5) Babaei, M.; Jalilian, M.; Shahbaz, K. Chemical Recycling of Polyethylene Terephthalate: A Mini-Review. *Journal of Environmental Chemical Engineering* **2024**, *12*, 112507.

(6) Singh, A.; Rorrer, N. A.; Nicholson, S. R.; Erickson, E.; DesVeaux, J. S.; Avelino, A. F. T.; Lamers, P.; Bhatt, A.; Zhang, Y.; Avery, G.; Tao, L.; Pickford, A. R.; Carpenter, A. C.; McGeehan, J. E.; Beckham, G. T. Techno-Economic, Life-Cycle, and Socioeconomic Impact Analysis of Enzymatic Recycling of Poly(Ethylene Terephthalate). *Joule* **2021**, *5*, 2479−2503.

(7) Joo, S.; Cho, I. J.; Seo, H.; Son, H. F.; Sagong, H. Y.; Shin, T. J.; Choi, S. Y.; Lee, S. Y.; Kim, K. J. Structural Insight into Molecular Mechanism of Poly(Ethylene Terephthalate) Degradation. *Nat. Commun.* **2018**, *9*, 382.

(8) Rauwerdink, A.; Kazlauskas, R. J. How the Same Core Catalytic Machinery Catalyzes 17 Different Reactions: The Serine-Histidine-Aspartate Catalytic Triad of Alpha/Beta-Hydrolase Fold Enzymes. *ACS Catal.* **2015**, *5*, 6153−6176.

(9) Jerves, C.; Neves, R. P. P.; Ramos, M. J.; da Silva, S.; Fernandes, P. A. Reaction Mechanism of the PET Degrading Enzyme Petase Studied with Dft/Mm Molecular Dynamics Simulations. *ACS Catal.* **2021**, *11*, 11626−11638.

(10) Hedstrom, L. Serine Protease Mechanism and Specificity. *Chem. Rev.* **2002**, *102*, 4501−24.

(11) Dodson, G.; Wlodawer, A. Catalytic Triads and Their Relatives. *Trends Biochem. Sci.* **1998**, *23*, 347−52.

(12) Baker, C. J. Cutin Degradation by Plant Pathogenic Fungi. *Phytopathology* **1978**, *68*, 1577.

(13) Yoshida, S.; Hiraga, K.; Takehana, T.; Taniguchi, I.; Yamaji, H.; Maeda, Y.; Toyohara, K.; Miyamoto, K.; Kimura, Y.; Oda, K. A Bacterium That Degrades and Assimilates Poly(Ethylene Terephthalate). *Science* **2016**, *351*, 1196−9.

(14) Tournier, V.; Topham, C. M.; Gilles, A.; David, B.; Folgoas, C.; Moya-Leclair, E.; Kamionka, E.; Desrousseaux, M. L.; Texier, H.; Gavalda, S.; Cot, M.; Guemard, E.; Dalibey, M.; Nomme, J.; Cioci, G.; Barbe, S.; Chateau, M.; Andre, I.; Duquesne, S.; Marty, A. An Engineered PET Depolymerase to Break Down and Recycle Plastic Bottles. *Nature* **2020**, *580*, 216−219.

(15) Then, J.; Wei, R.; Oeser, T.; Barth, M.; Belisario-Ferrari, M. R.; Schmidt, J.; Zimmermann, W. Ca2+ and Mg2+ Binding Site Engineering Increases the Degradation of Polyethylene Terephthalate Films by Polyester Hydrolases from *Thermobifida Fusca*. *Biotechnol J.* **2015**, *10*, 592−8.

(16) Kawai, F.; Oda, M.; Tamashiro, T.; Waku, T.; Tanaka, N.; Yamamoto, M.; Mizushima, H.; Miyakawa, T.; Tanokura, M. A Novel Ca(2)(+)-Activated, Thermostabilized Polyesterase Capable of Hydrolyzing Polyethylene Terephthalate from *Saccharomonospora Viridis* Ahk190. *Appl. Microbiol. Biotechnol.* **2014**, *98*, 10053−64.

(17) Sulaiman, S.; Yamato, S.; Kanaya, E.; Kim, J. J.; Koga, Y.; Takano, K.; Kanaya, S. Isolation of a Novel Cutinase Homolog with Polyethylene Terephthalate-Degrading Activity from Leaf-Branch Compost by Using a Metagenomic Approach. *Appl. Environ. Microbiol.* **2012**, *78*, 1556−62.

(18) Kan, Y.; He, L.; Luo, Y.; Bao, R. Ispetase Is a Novel Biocatalyst for Poly(Ethylene Terephthalate) (PET) Hydrolysis. *Chembiochem* **2021**, *22*, 1706−1716.

(19) Danso, D.; Schmeisser, C.; Chow, J.; Zimmermann, W.; Wei, R.; Leggewie, C.; Li, X.; Hazen, T.; Streit, W. R. New Insights into the Function and Global Distribution of Polyethylene Terephthalate (PET)-Degrading Bacteria and Enzymes in Marine and Terrestrial

Metagenomes. *Appl. Environ. Microbiol.* **2018**, *84*, DOI: 10.1128/AEM.02773-17.
(20) Meilleur, C.; Hupe, J. F.; Juteau, P.; Shareck, F. Isolation and Characterization of a New Alkali-Thermostable Lipase Cloned from a Metagenomic Library. *J. Ind. Microbiol. Biotechnol.* **2009**, *36*, 853−61.
(21) Chen, C.-C.; Han, X.; Li, X.; Jiang, P.; Niu, D.; Ma, L.; Liu, W.; Li, S.; Qu, Y.; Hu, H.; Min, J.; Yang, Y.; Zhang, L.; Zeng, W.; Huang, J.-W.; Dai, L.; Guo, R.-T. General Features to Enhance Enzymatic Activity of Poly(Ethylene Terephthalate) Hydrolysis. *Nature Catalysis* **2021**, *4*, 425−430.
(22) Han, X.; Liu, W.; Huang, J. W.; Ma, J.; Zheng, Y.; Ko, T. P.; Xu, L.; Cheng, Y. S.; Chen, C. C.; Guo, R. T. Structural Insight into Catalytic Mechanism of PET Hydrolase. *Nat. Commun.* **2017**, *8*, 2106.
(23) Chen, C. C.; Han, X.; Ko, T. P.; Liu, W.; Guo, R. T. Structural Studies Reveal the Molecular Mechanism of PETase. *FEBS J.* **2018**, *285*, 3717−3723.
(24) Crnjar, A.; Grinen, A.; Kamerlin, S. C. L.; Ramirez-Sarmiento, C. A. Conformational Selection of a Tryptophan Side Chain Drives the Generalized Increase in Activity of PET Hydrolases through a Ser/Ile Double Mutation. *ACS Org. Inorg. Au* **2023**, *3*, 109−119.
(25) Burgin, T.; Pollard, B. C.; Knott, B. C.; Mayes, H. B.; Crowley, M. F.; McGeehan, J. E.; Beckham, G. T.; Woodcock, H. L. The Reaction Mechanism of the *Ideonella Sakaiensis* PETase Enzyme. *Commun. Chem.* **2024**, *7*, 65.
(26) Nakamura, A.; Kobayashi, N.; Koga, N.; Iino, R. Positive Charge Introduction on the Surface of Thermostabilized PET Hydrolase Facilitates PET Binding and Degradation. *ACS Catal.* **2021**, *11*, 8550−8564.
(27) Singh, R.; Kumar, M.; Mittal, A.; Mehta, P. K. Microbial Enzymes: Industrial Progress in 21st Century. *3 Biotech* **2016**, *6*, 174.
(28) Wu, H.; Chen, Q.; Zhang, W.; Mu, W. Overview of Strategies for Developing High Thermostability Industrial Enzymes: Discovery, Mechanism, Modification and Challenges. *Crit Rev. Food Sci. Nutr* **2023**, *63*, 2057−2073.
(29) Selles Vidal, L.; Isalan, M.; Heap, J. T.; Ledesma-Amaro, R. A Primer to Directed Evolution: Current Methodologies and Future Directions. *RSC Chem. Biol.* **2023**, *4*, 271−291.
(30) Wei, R.; von Haugwitz, G.; Pfaff, L.; Mican, J.; Badenhorst, C. P. S.; Liu, W.; Weber, G.; Austin, H. P.; Bednar, D.; Damborsky, J.; Bornscheuer, U. T. Mechanism-Based Design of Efficient PET Hydrolases. *ACS Catal.* **2022**, *12*, 3382−3396.
(31) Zhong-Johnson, E. Z. L.; Voigt, C. A.; Sinskey, A. J. An Absorbance Method for Analysis of Enzymatic Degradation Kinetics of Poly(Ethylene Terephthalate) Films. *Sci. Rep* **2021**, *11*, 928.
(32) He, F. Y.; Wang, L. F.; Li, B. R.; Wang, Q. G.; Wang, Q. Studies on Crystal Structure and Hydrolysis Feature of the Fluorescein Dibenzoate. *Acta Chim. Sin.* **1993**, *51*, 119−124.
(33) Qiao, Y.; Hu, R.; Chen, D.; Wang, L.; Wang, Z.; Yu, H.; Fu, Y.; Li, C.; Dong, Z.; Weng, Y. X.; Du, W. Fluorescence-Activated Droplet Sorting of PET Degrading Microorganisms. *J. Hazard Mater.* **2022**, *424*, 127417.
(34) Wei, R.; Oeser, T.; Barth, M.; Weigl, N.; Lübs, A.; Schulz-Siegmund, M.; Hacker, M. C.; Zimmermann, W. Turbidimetric Analysis of the Enzymatic Hydrolysis of Polyethylene Terephthalate Nanoparticles. *Journal of Molecular Catalysis B: Enzymatic* **2014**, *103*, 72−78.
(35) Belisario-Ferrari, M. R.; Wei, R.; Schneider, T.; Honak, A.; Zimmermann, W. Fast Turbidimetric Assay for Analyzing the Enzymatic Hydrolysis of Polyethylene Terephthalate Model Substrates. *Biotechnol J.* **2019**, *14*, No. e1800272.
(36) Richter, P. K.; Blazquez-Sanchez, P.; Zhao, Z.; Engelberger, F.; Wiebeler, C.; Kunze, G.; Frank, R.; Krinke, D.; Frezzotti, E.; Lihanova, Y.; Falkenstein, P.; Matysik, J.; Zimmermann, W.; Strater, N.; Sonnendecker, C. Structure and Function of the Metagenomic Plastic-Degrading Polyester Hydrolase PHL7 Bound to Its Product. *Nat. Commun.* **2023**, *14*, 1905.
(37) Cui, Y.; Chen, Y.; Sun, J.; Zhu, T.; Pang, H.; Li, C.; Geng, W. C.; Wu, B. Computational Redesign of a Hydrolase for Nearly Complete Pet Depolymerization at Industrially Relevant High-Solids Loading. *Nat. Commun.* **2024**, *15*, 1417.
(38) Choi, J. H.; Lee, S. Y. Secretory and Extracellular Production of Recombinant Proteins Using *Escherichia Coli*. *Appl. Microbiol. Biotechnol.* **2004**, *64*, 625−35.
(39) Su, L.; Woodard, R. W.; Chen, J.; Wu, J. Extracellular Location of *Thermobifida Fusca* Cutinase Expressed in *Escherichia Coli* Bl21(D3) without Mediation of a Signal Peptide. *Appl. Environ. Microbiol.* **2013**, *79*, 4192−8.
(40) Shirke, A. N.; White, C.; Englaender, J. A.; Zwarycz, A.; Butterfoss, G. L.; Linhardt, R. J.; Gross, R. A. Stabilizing Leaf and Branch Compost Cutinase (LCC) with Glycosylation: Mechanism and Effect on Pet Hydrolysis. *Biochemistry* **2018**, *57*, 1190−1200.
(41) Seo, H.; Kim, S.; Son, H. F.; Sagong, H. Y.; Joo, S.; Kim, K. J. Production of Extracellular Petase from *Ideonella Sakaiensis* Using Sec-Dependent Signal Peptides in *E. Coli*. *Biochem. Biophys. Res. Commun.* **2019**, *508*, 250−255.
(42) Kadokura, K.; Sakamoto, Y.; Saito, K.; Ikegami, T.; Hirano, T.; Hakamata, W.; Oku, T.; Nishio, T. Production and Secretion of a Recombinant *Vibrio Parahaemolyticus* Chitinase by *Escherichia Coli* and Its Purification from the Culture Medium. *Biosci Biotechnol Biochem* **2007**, *71*, 2848−51.
(43) Xi, X.; Ni, K.; Hao, H.; Shang, Y.; Zhao, B.; Qian, Z. Secretory Expression in *Bacillus Subtilis* and Biochemical Characterization of a Highly Thermostable Polyethylene Terephthalate Hydrolase from Bacterium Hr29. *Enzyme Microb Technol.* **2021**, *143*, 109715.
(44) Cui, Y.; Chen, Y.; Liu, X.; Dong, S.; Tian, Y. e.; Qiao, Y.; Mitra, R.; Han, J.; Li, C.; Han, X.; Liu, W.; Chen, Q.; Wei, W.; Wang, X.; Du, W.; Tang, S.; Xiang, H.; Liu, H.; Liang, Y.; Houk, K. N.; Wu, B. Computational Redesign of a PETase for Plastic Biodegradation under Ambient Condition by the Grape Strategy. *ACS Catal.* **2021**, *11*, 1340−1350.
(45) Bell, E. L.; Smithson, R.; Kilbride, S.; Foster, J.; Hardy, F. J.; Ramachandran, S.; Tedstone, A. A.; Haigh, S. J.; Garforth, A. A.; Day, P. J. R.; Levy, C.; Shaver, M. P.; Green, A. P. Directed Evolution of an Efficient and Thermostable PET Depolymerase. *Nature Catalysis* **2022**, *5*, 673−681.
(46) Cribari, M. A.; Unger, M. J.; Unarta, I. C.; Ogorek, A. N.; Huang, X.; Martell, J. D. Ultrahigh-Throughput Directed Evolution of Polymer-Degrading Enzymes Using Yeast Display. *J. Am. Chem. Soc.* **2023**, *145*, 27380−27389.
(47) Joho, Y.; Royan, S.; Caputo, A. T.; Newton, S.; Peat, T. S.; Newman, J.; Jackson, C.; Ardevol, A. Enhancing PET Degrading Enzymes: A Combinatory Approach. *Chembiochem* **2024**, *25*, No. e202400084.
(48) Ding, Z.; Xu, G.; Miao, R.; Wu, N.; Zhang, W.; Yao, B.; Guan, F.; Huang, H.; Tian, J. Rational Redesign of Thermophilic PET Hydrolase LCCICCG to Enhance Hydrolysis of High Crystallinity Polyethylene Terephthalates. *J. Hazard Mater.* **2023**, *453*, 131386.
(49) Jumper, J.; Evans, R.; Pritzel, A.; Green, T.; Figurnov, M.; Ronneberger, O.; Tunyasuvunakool, K.; Bates, R.; Zidek, A.; Potapenko, A.; Bridgland, A.; Meyer, C.; Kohl, S. A. A.; Ballard, A. J.; Cowie, A.; Romera-Paredes, B.; Nikolov, S.; Jain, R.; Adler, J.; Back, T.; Petersen, S.; Reiman, D.; Clancy, E.; Zielinski, M.; Steinegger, M.; Pacholska, M.; Berghammer, T.; Bodenstein, S.; Silver, D.; Vinyals, O.; Senior, A. W.; Kavukcuoglu, K.; Kohli, P.; Hassabis, D. Highly Accurate Protein Structure Prediction with Alphafold. *Nature* **2021**, *596*, 583−589.
(50) Peter Eastman, J. S.; Chodera, J.; McGibbon, R. T.; Simmonett, A.; Sherman, M.; et al.. *Openmm/Openmm: Openmm 8.1.1* (8.1.1); Zenodo, 2024.
(51) Wang, L. P.; Martinez, T. J.; Pande, V. S. Building Force Fields: An Automatic, Systematic, and Reproducible Approach. *J. Phys. Chem. Lett.* **2014**, *5*, 1885−91.
(52) Humphrey, W.; Dalke, A.; Schulten, K. Vmd: Visual Molecular Dynamics. *J. Mol. Graph* **1996**, *14*, 33−8.

https://doi.org/10.1021/acsomega.4c05488
ACS Omega 2024, 9, 34151−34160